

Improved graphene blisters by ultra-high pressure sealing

Y. Manzanares-Negro¹, P. Ares^{1†}, M. Jaafar¹, G. López-Polín^{1‡}, C. Gómez-Navarro^{1,2}, J. Gómez-Herrero^{1,2}

¹Departamento de Física de la Materia Condensada. Universidad Autónoma de Madrid, 28049, Madrid, Spain.

²Condensed Matter Physic Center IFIMAC. Universidad Autónoma de Madrid, 28049, Madrid, Spain.

[†]Present affiliation: School of Physics & Astronomy and National Graphene Institute, University of Manchester. Manchester M13 9PL, UK.

[‡]Department of physics. Freie University, Berlin. Kaiserswerther Str. 16-18, 14195 Berlin, Germany.

Abstract

We report the diffusion of air from pressurized graphene drumheads and propose a method to improve the already ultrastrong adhesion between graphene and the underlying SiO₂ substrate. This is carried out by applying controlled and localized ultrahigh pressure (> 10 GPa) with an Atomic Force Microscopy diamond tip. With this procedure, we are able to significantly approach the graphene to the surface around the drumheads, allowing us to better seal the graphene-SiO₂ interface, which is reflected in a drop of the leakage time in a factor of ~4. An additional implication of our work is that gas flow through the graphene-SiO₂ interface contributes significantly to the total leak rate. Our work opens a way to improve the performance of graphene as a gas membrane.

Even though it is only one atom thick, due to its defect free nature, graphene shows great impermeability[1] and seems to be the ideal candidate to enclose even the smallest gas molecules.[2] The standard setup used to exploit this extreme impermeability is based on the creation of an open micro-cavity within other bulk material (usually SiO₂) that is subsequently covered by a graphene layer acting as a drum head (see Figure 1a for a schematic view). This configuration has been already proved useful for applications such as graphene microphones[3],[4] pressure sensors[5] or tunable systems to confine charge carriers.[6] In addition, these graphene blisters have been used in fundamental research experiments with the aim of determining mechanical magnitudes such as elastic modulus[1] or graphene permeability to different gases.[7]

The good performance (high impermeability) of such devices relies on a very high adhesive interaction between the graphene layer and the underlying material. In a pioneer work by Bunch *et al.*[8] the adhesion energy of monolayer graphene and SiO₂ was reported to be 0.45 J/m². This anomalously high figure is attributed to the extreme flexibility of graphene, which allows it to conform to the topography of the underlying material, maximizing surface adhesion. However, this upper bound value of adhesion energy is usually not reached in most samples, and lower adhesion energies and higher leakage rates are usually measured.[9, 10]

Although the presence of wrinkles and folds in graphene or residue in the graphene-substrate interface are known to highly modify adhesion energy, it is still not clear whether the origin of pressure equilibration in graphene blisters comes from diffusion of gas molecules through the SiO₂ or through the graphene-SiO₂ interface.[1] Unraveling this issue is crucial for stable measurements since the reported leakage rates would mean that a typical cavity with dimensions of 1 x 1 x 0.5 microns under a pressure difference of 4 bar would lose 50% pressure in just a few hours.

In this work, we first report experimental evidence indicating that the diffusion of molecules through the graphene-SiO₂ interface is the predominant mechanism for gas leak in graphene-SiO₂ cavities (at least for medium molecules such as N₂). We then propose a simple technique that improves significantly the cavity sealing. It is based on the application of very local ultrahigh pressure (> 10 GPa) on a nanometer wide rim surrounding the cavity by means of an Atomic Force Microscopy (AFM) diamond tip.[11] With this technique we have been able to improve the leak characteristic time of our micro-cavities up to a factor of ~4, confirming that diffusion through the interface is crucial for sealing these micro-cavities.

We prepared graphene micro-cavities by mechanical exfoliation of natural graphite on SiO₂ (300 nm)/Si substrates with predefined circular wells of diameters ranging from 0.5 to 3 μm. We selected only flat (unfolded, unwrinkled) monolayer graphene flakes for this study. AFM images of the drumheads revealed that, as reported previously, graphene layers adhere to the vertical walls of the wells for ~2-10 nm in depth in their initial morphology.[12, 13] We carried out all the experiments described in this work in a variable pressure chamber equipped with an Atomic Force Microscope.[14] By controlling the internal pressure in the micro-cavity (P_{in}) and external pressure within this chamber (P_{out}), we are able to apply a pressure difference of up to 4 atm to our graphene blisters for convex geometry ($P_{out} > P_{in}$) and almost 1 atm for concave geometry ($P_{out} < P_{in}$). See figure 1a for a schematic view. Once a pressure difference is applied through the cavity, we acquire consecutive AFM topography images in dynamic mode in the same area for long (hours-days) periods of time. All the experiments presented herein used N₂ or air as filling gas obtaining similar results.

Figure 1a shows a scheme of the possible configurations of the blisters according to the different combinations of P_{in} and P_{out} (top panel) together with representative AFM topographies (bottom panel). For a blister where the pressures are equilibrated ($P_{in} = P_{out}$) (figure 1a, left), the flake appears flat, slightly adhered to the well. In the case of a blister that initially supports an internal pressure higher than the external one ($P_{in} > P_{out}$) (figure 1a, middle), the flake deflects outwards *i.e.* concave geometry. If the pressure is applied in the opposite direction $P_{in} < P_{out}$ (figure 1a, right) the graphene membrane deflects inwards *i.e.* convex geometry. In what follows, we define $\Delta P = P_{in} - P_{out}$, thus $\Delta P > 0$ implies concave blister shape and $\Delta P < 0$ convex. By monitoring the maximum/minimum positions (extrema) of the blister through AFM images (see figure 1b), we always observe that, in absolute value, they always decrease with time, implying that the pressure difference across the membrane tends to equilibrate. For these experiments it is important to remark that what we can measure from the AFM topographies is the blister shape and not the pressure inside the well. We fix an initial ΔP in the cavity and then we approach the AFM tip to the surface. This process usually takes a few minutes, along this time the gas is already flowing from/to the microchamber as it tends to reduce the absolute value of ΔP . This implies that when we finish the first AFM image the blister ΔP is unknown, hence the observable is the extrema of the blister. Thus, all the values for ΔP considered in this work are values for the initial pressure difference that we set in the macroscopic chamber. Importantly, ΔP and the maximum/minimum deflection of the blister are related through a potential law $\Delta P \sim \Delta z^3_{extrema}$. [1]

Figure 1c presents the evolution of the extrema for the blister in figures 1 a and b, for two opposite pressure differences (+1 atm, top panel and -1 atm, bottom panel). Here we can appreciate how the extrema evolve with time towards zero (flat membrane). However, the evolution for the concave geometry is faster than for the convex one. To quantify this time we have heuristically fitted the experimental data to an exponential decay curve $\Delta z(t) = z_0 \cdot e^{-t/\tau}$ being z_0 the initial extrema of the blisters, and τ a characteristic time, obtaining values of 345 min for concave geometry ($\Delta P > 0$) and 540 min for the convex one ($\Delta P < 0$) for the same blister. The fact that τ is higher for $\Delta P < 0$ suggests that the shape of the membrane with respect to the SiO_2 substrate, and hence the graphene- SiO_2 interaction, has a marked influence on the leakage rate, in contradiction with what is expected for a pressure equilibrium mechanism dominated by diffusion through SiO_2 .

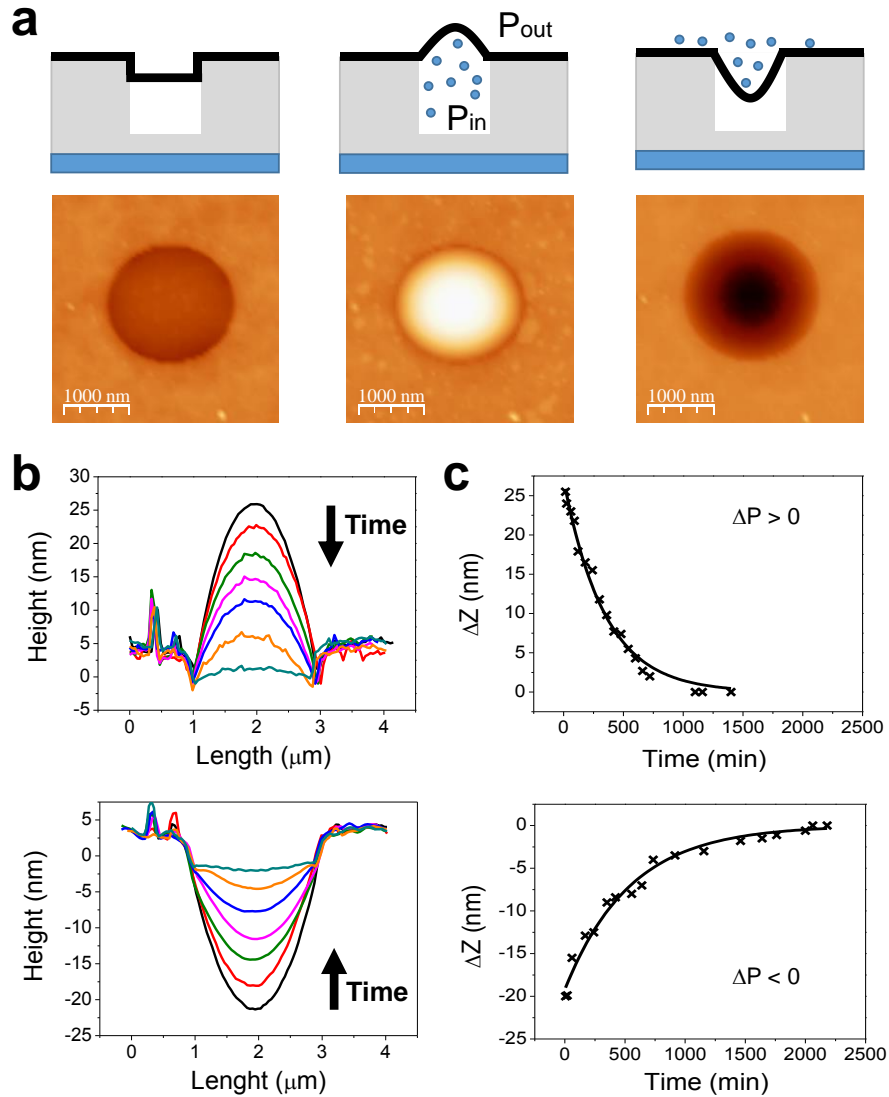


Figure 1. Leakage rate for two different blister configurations. (a) Schematic view (top) and corresponding AFM topographical images (bottom) of the possible configurations. (b) AFM line traces taken through the center of the graphene membrane of (a). (c) Time evolution of the blister extrema positions when the internal pressure is higher than the external, $\Delta P = +1$ atm (top) and when the internal pressure is lower than the external, $\Delta P = -1$ atm (bottom). Fitting to an exponential decay yields characteristic times of 345 and 540 min respectively.

We have also observed that the leakage rate is different for different cavities and from one flake to other. These variations can be attributed to a combination of different factors such as uncontrolled tensions, atomic sized ripples or folds,[15] surface contamination and the distance of the microchamber to the closest graphene flake edge. Whereas it is experimentally challenging to account for the contribution of wrinkles and contamination, Figure 2 presents a comparison of leakage rates for different blisters of the same dimensions formed with the same graphene flake. Figure 2a portrays an optical microscopy image where a graphene flake covers the substrate forming several microchambers. Here we will focus on 3 different cavities (marked with square, circle and triangle) with the same diameter but different distance to the graphene edge. Figures 2b and c show the evolution of the extrema positions of the

membrane as a function of time for the three wells above mentioned. The symbols in the plot correspond to the polygons used in figure 2a, leading to characteristic times for the concave geometry ($\Delta P > 0$) of $\tau \approx 175, 340$ and 365 min for squares, circles and triangles respectively and $310, 755$ and 855 min for the convex one ($\Delta P < 0$). For all cases the characteristic times are higher for $\Delta P < 0$. The different τ for each of the geometries reflects the distance from each well to the edge of the flake. This is clearly observed in figure 2d where we represent a plot of the characteristic times for different wells in the flake as a function of the distance to the edge of the flake.

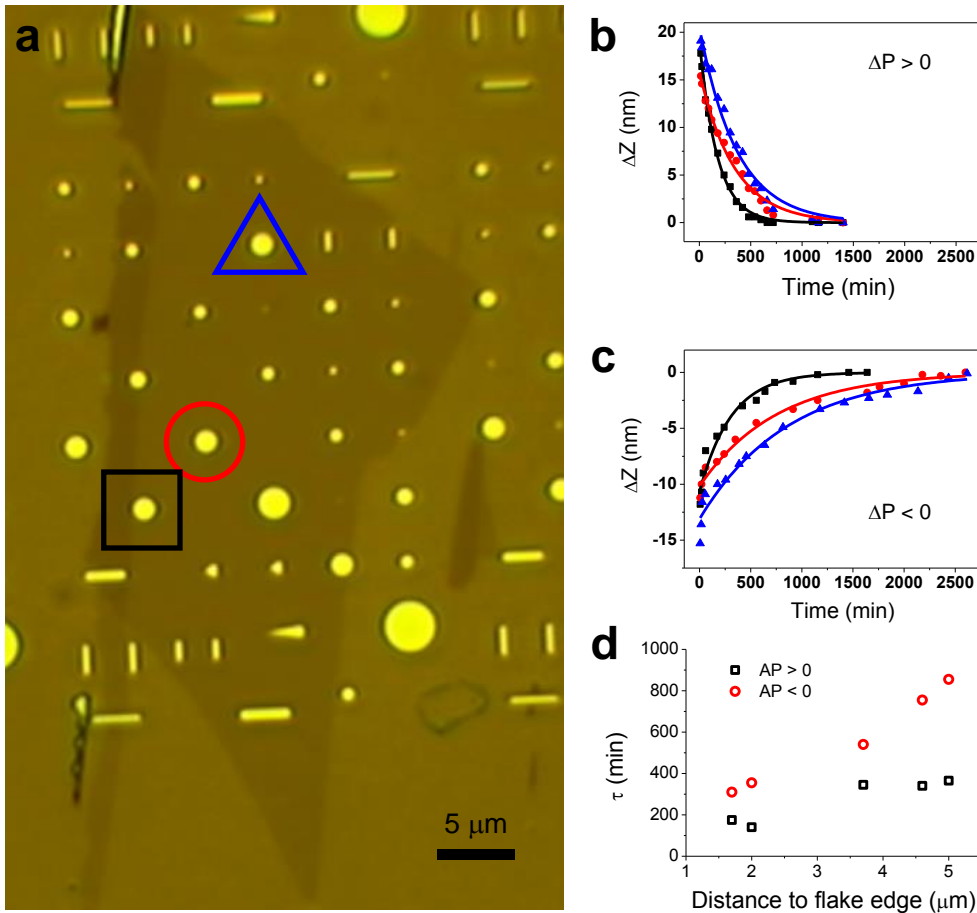


Figure 2. Comparison of leakage rates for different blisters. (a) Optical image of a graphene flake (mostly one layer) obtained by microexfoliation on a substrate with holes. (b) Time evolution of the blister maximum position for the holes ($1.5 \mu\text{m}$ in diameter) surrounded by polygons in (a) when the initial pressure inside the microchambers is higher than the external pressure ($\Delta P = +1 \text{ atm}$). Fitting to an exponential drop yields characteristic times of 175, 340 and 365 min for square, circle and triangle data respectively. (c) Same as in (b) but now with an initial internal pressure lower than the external ($\Delta P = -1 \text{ atm}$). In this case the minimum position of the blisters is represented and $\tau \approx 310, 755$ and 855 min for square, circle and triangle data are found respectively. (d) Characteristic times as a function of the distance to the flake edge for several blisters in (a).

In order to improve the sealing of the microcavities we have developed a method based on applying ultrahigh pressure with an AFM diamond tip. This method takes advantage of the extremely high breaking strength of graphene that allows applying ultrahigh pressure without damaging neither the flake nor the substrate.[16],[17] It involves the following steps, as depicted in Figure 3: first we carry out a non-invasive gentle AFM image of the flake in dynamic mode (Figure 3a). Then, we apply a load corresponding to a pressure between 20 and 35 GPa on a selected area with the shape of a nanometric wide rim surrounding the desired cavity (see a schematic view in Figure 3b). Finally, we go back to dynamic mode conditions and acquire a new topography image (Figure 3c). Comparing both images we can clearly distinguish the depression on graphene created during the pressure load. A profile along the green line in figure 3c depicts the ~ 1 nm depth of this area (Figure 3d). This depression in height can be attributed to an approach of graphene to the substrate. Lower pressures yielded unnoticeable changes and higher pressures yielded graphene fracture. Further details can be found in our previous work.[11]

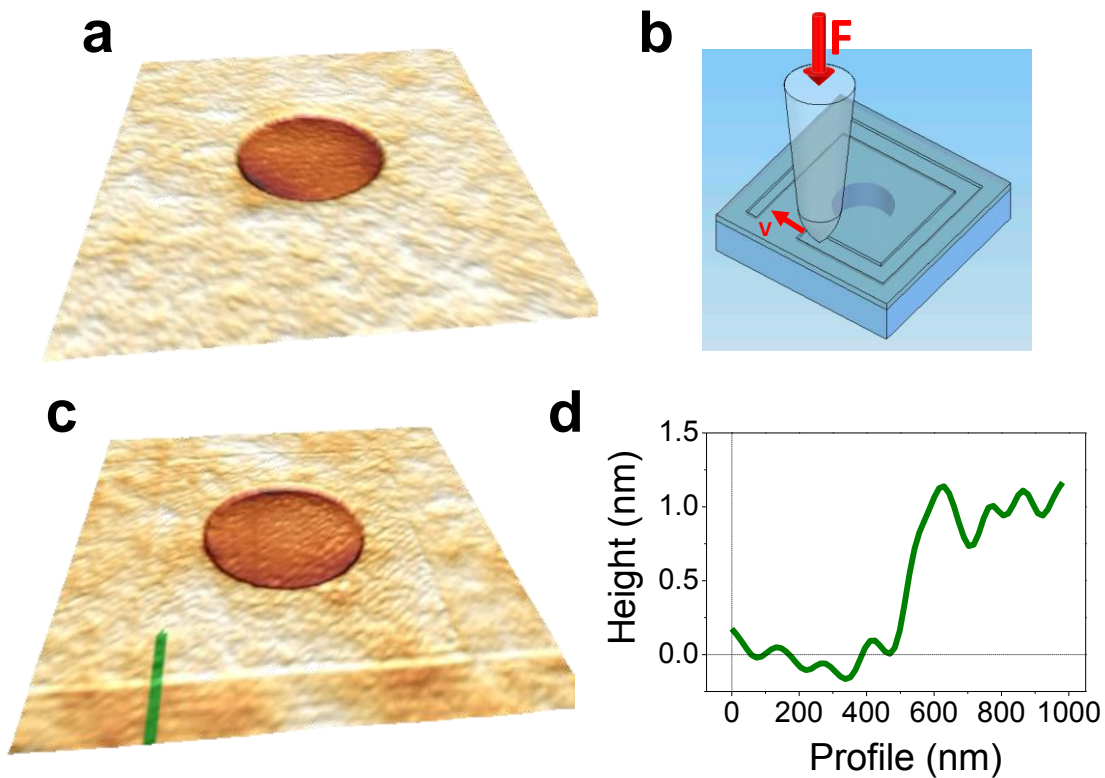


Figure 3. Sealing microchambers. (a) AFM topography showing a $1.5 \mu\text{m}$ diameter well covered by a monolayer graphene flake. (b) Schematic of the process to improve the sealing: a diamond tip scans in hard contact the flake surrounding the well. (c) AFM topography showing the result of the sealing process. (d) Profile along the green line in (c). The depth of the depressed region is about 1 nm.

We have applied this procedure to different blisters both for concave and convex configurations. Figure 4 presents the evolution of the extrema for representative graphene microchambers before and after sealing. While the characteristic time for a blister subjected to

an initial $\Delta P = +1$ atm was $\tau = 40$ min, after sealing this time increases to 75 min (Figure 4a). For a blister with a pressure difference $\Delta P = -4$ atm (Figure 4b), the characteristic time increases from 40 to 140 min, almost by a factor of 4. It is worth to remark that we have been able to increase the characteristic leakage time both in concave and convex configurations.

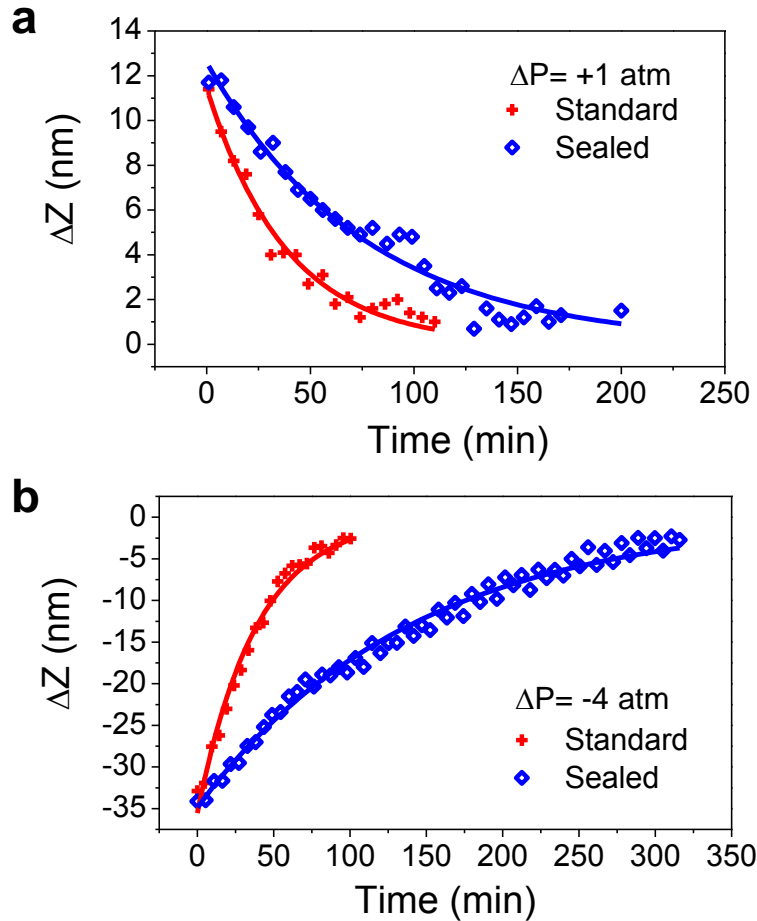


Figure 4. Comparison of leakage rates before and after sealing. (a) Time evolution of the maximum position for a blister with $\Delta P > 0$ in the standard (unsealed, crosses) and sealed (diamonds) cases. The characteristic times are $\tau = 40$ and 75 min respectively. (b) Same as in (a) but now for a well with $\Delta P < 0$. The characteristic times in this case are $\tau = 40$ and 140 min for the standard and sealed cases respectively.

To sum up, we measure the leakage rate for graphene blisters concluding that the main contribution to this magnitude is gas flow through the graphene/substrate interface. We also demonstrate that the leakage rate can be substantially reduced by sealing the blister using an AFM diamond tip. This method is particularly relevant for flakes with a poor adhesion, such as those placed on the substrate using a transfer procedure.

References

1. Bunch, J.S., et al., *Impermeable atomic membranes from graphene sheets*. Nano Letters, 2008. **8**(8): p. 2458-2462.
2. Koenig, S.P., et al., *Selective molecular sieving through porous graphene*. Nature Nanotechnology, 2012. **7**(11): p. 728-732.
3. Todorovic, D., et al., *Multilayer graphene condenser microphone*. 2d Materials, 2015. **2**(4).
4. Zhou, Q. and A. Zettl, *Electrostatic graphene loudspeaker*. Applied Physics Letters, 2013. **102**(22).
5. Smith, A.D., et al., *Piezoresistive Properties of Suspended Graphene Membranes under Uniaxial and Biaxial Strain in Nanoelectromechanical Pressure Sensors*. ACS Nano, 2016. **10**(11): p. 9879-9886.
6. Abdullah, H.M., et al., *Graphene quantum blisters: A tunable system to confine charge carriers*. Applied Physics Letters, 2018. **112**(21).
7. Koenig, S.P., et al., *Selective molecular sieving through porous graphene*. Nature Nanotechnology, 2012. **7**(11): p. 728-732.
8. Koenig, S.P., et al., *Ultrastrong adhesion of graphene membranes*. Nature Nanotechnology, 2011. **6**(9): p. 543-546.
9. Suk, J.W., et al., *Probing the adhesion interactions of graphene on silicon oxide by nanoindentation*. Carbon, 2016. **103**: p. 63-72.
10. Wood, J.D., C.M. Harvey, and S. Wang, *Adhesion toughness of multilayer graphene films*. Nature Communications, 2017. **8**.
11. Ares P., e.al., *Ultrahigh Pressure Local Tuning of Graphene Electronic Properties. To be published*.
12. Lee, C., et al., *Measurement of the elastic properties and intrinsic strength of monolayer graphene*. Science, 2008. **321**(5887): p. 385-388.
13. Lopez-Polin, G., et al., *Increasing the elastic modulus of graphene by controlled defect creation*. Nature Physics, 2015. **11**(1): p. 26-31.
14. Lopez-Polin, G., et al., *The influence of strain on the elastic constants of graphene*. Carbon, 2017. **124**: p. 42-48.
15. Choi, J.S., et al., *Friction Anisotropy-Driven Domain Imaging on Exfoliated Monolayer Graphene*. Science, 2011. **333**(6042): p. 607-610.
16. Lee, C., et al., *Measurement of the elastic properties and intrinsic strength of monolayer graphene*. Science, 2008. **321**(5887): p. 385-388.
17. Vasic, B., et al., *Nanoscale wear of graphene and wear protection by graphene*. Carbon, 2017. **120**: p. 137-144.